IJICT International Journal of Information & Communication Technology
ITRC
Volume 1- Number 2- May 2009 (pp.1-11)

Novel Approach to Ultra-Wideband Antenna Design

Kian Paran
Communications Technology Institute
Iran Telecommunication Research Center
Tehran, Iran
kianparan@itrc.ac.ir

Masoum Fardis
Communications Technology Institute
Iran Telecommunication Research Center
Tehran, Iran
fardis@itrc.ac.ir

Ali Abolghasemi
Communications Technology Institute
Iran Telecommunication Research Center
Tehran, Iran
ali_abl@itrc.ac.ir

Received: December 13, 2008- Accepted: April 21, 2009

***Abstract*— A novel approach to ultra-wideband (UWB) antenna design is presented which is based on a general description for the geometry of monopole antennas. This general description is capable of producing almost all possible shapes for monopole antennas and it is compatible with different optimization methods. The general description is used for the optimization of rotationally-symmetric monopole antenna with finite ground plane. The optimization of antennas is performed by applying a hybrid procedure, which begins with a global search and completes with a local optimization. The optimization procedure aims at minimizing the reflection from antennas while reducing the distortion of radiated pulses. In some cases, the reduction of variations in the energy pattern is also considered. The numerical results show the reliability and effectiveness of the whole process and considerable improvement in comparison with similar antennas reported in the literature.**

Keywords-Genetic algorithm (GA), Monopole antenna, Optimization, Spline, Time-domain analysis, Ultra-wideband (UWB) antennas

چکیده – در این نوشته روشی نو در طراحی آنتن‌های فراپهن‌باند ارائه می‌گردد که بر پایهٔ توصیفی فراگیر برای شکل هندسی آنتن‌های تک‌قطبی می‌باشد. این توصیف فراگیر توانایی ساختن کمابیش همهٔ شکل‌های ممکن برای آنتن‌های تک‌قطبی را داراست و با روش‌های گوناگون بهینه‌سازی سازگار می‌باشد. در این پژوهش، این توصیف فراگیر برای بهینه‌سازی آنتن‌های تک‌قطبی دارای تقارن گردشی با صفحهٔ زمین محدود بکارگرفته شده است. بهینه‌سازی آنتن‌ها با بکاربستن روندی دو مرحله‌ای به انجام می‌رسد که با بهینه‌سازی فراگیر آغاز و با بهینه‌سازی محلی تکمیل می‌گردد. روند بهینه‌سازی به آماج کمینه نمودن بازتاب از آنتن‌ها به همراه کاهش اعوجاج پالس‌های تابشی انجام می‌گیرد. در برخی موردها کاهش تغییر در الگوی تابشی انرژی نیز یکی از آماج‌های بهینه‌سازی می‌باشد. نتیجه‌های عددی نشان‌دهندهٔ استواری و کارایی سراسر فرایند و همچنین نشان‌دهندهٔ بهبود چشمگیر کارکرد آنتن‌ها در همسنجی با آنتن‌های همانند گزارش‌شده می‌باشد.

I. Introduction

Since the allocation of the 3.1-10.6 GHz spectrum by the Federal Communications Commission (FCC) for ultra-wideband (UWB) radio applications [1], the interest in this technology has increased greatly. Attractive features like immunity to interferences and noise, extremely low emission levels, and high-speed data transmission make the UWB a promising technology. Potential applications of UWB range from wireless communications and measurement to various types of radar, imaging, and medical systems [1]. In UWB radio systems, unlike conventional narrowband ones, antennas are transmitting or receiving sub-nanosecond base-band pulses. Consequently, the traditional frequency-domain description and characterization of antennas behavior and performance are not adequate for UWB antennas. Therefore, the selection and design of antennas for UWB systems should be accomplished in a comprehensive manner taking into account not only the impedance matching over the operating band, but also the time-domain distortion of pulses and pattern characteristics [2], [3].

Monopole and dipole antennas due to their small size, omnidirectional radiation pattern, versatility, and flexibility are suitable for many UWB applications. Numerous designs for UWB monopole and dipole antennas have been proposed in literature. Planar and non-planar antennas with different shapes (including triangular, rectangular, trapezoidal, hexagonal, circular, elliptical, spherical, conical, and more complicated geometries) have been examined [4]-[8]. The optimization of UWB monopole and dipole antennas are mostly done by choosing a particular shape and tuning the geometrical parameters of it [9]-[11]. In few works, optimization has been performed not to obtain the optimum parameters of a particular shape, but to find the optimal shape of antenna [12]-[14]. In these works, the geometry of antennas is described in a general manner allowing the antennas to take different shapes during the optimization process. However, none of these general descriptions could produce all or most of the shapes for UWB monopole and dipole antennas which have been reported in the literature. Some of these general descriptions are also incompatible with some optimization methods like genetic algorithm (GA). For example, the crossover between two acceptable shapes may generate one or two unacceptable (e.g. self-intersecting) shapes.

In this paper, a novel approach to UWB antenna design is described. This approach is based on a general description for the geometry of UWB monopole antennas which is capable of producing almost all possible shapes for these antennas. This general description is also compatible with different optimization methods (especially GA). In this work, the general description is used for the optimization of non-planar rotationally-symmetric monopole antenna with finite ground plane. The rotational symmetry of structure and excitation makes the antenna pattern precisely omnidirectional and cancels the crosspolarization.

II. Optimization Process

During the optimization process, the "optimization tool" generates set or sets of parameters at each iteration. Each set of parameters corresponds to an antenna according to the "general description of antennas geometry". Antennas are analyzed using an "electromagnetic simulator" and for each antenna, the value of objective function is calculated. This value reversely shows the fitness of the antenna with regard to the optimization goals. At subsequent iterations, the optimization tool uses these values and the corresponding sets of parameters to generate new sets of parameters which are expected to exhibit better fitness. The key parts of the optimization setup are discussed in this section.

A. General Description of Antennas Geometry

The proposed scheme to generally describe the geometry of a rotationally-symmetric monopole antenna with finite ground plane is illustrated in Fig. 1. The primary profile of the antenna is formed by 12 control points, 4 points for shaping the ground (U_0-U_3), 4 points for shaping the lower part of radiating element (V_0-V_3), and 4 points for shaping the upper part of radiating element (W_0-W_3). The final profile consists of one rectangle (the cross-section of lower plate) and two splines (one forming the cross-section of shaped ground and the other forming the cross-section of radiating element). In Fig. 1, a, b, c, and l are the geometrical parameters of the feeding coaxial line and t is the thickness of lower plate. Moreover, $\Delta\rho_{max}$ is the maximum allowable distance between the control points and the outer conductor of coaxial line, Δz_{max} is the maximum allowable distance between control points and ρ –axis, $\Delta\rho_{grd}$ is the maximum allowable range for ground plane to extend beyond the shaped part, $\Delta\rho_{mar}$ is the margin along the ρ – direction, and Δz_{mar} is the margin along the z – direction.

The first control point of the ground (U_0) is positioned along the outer conductor of coaxial line ($\rho = b$), the first control point of the lower part of radiating element (V_0) is positioned along the inner conductor of coaxial line ($\rho = a$), and the first control point of the upper part of radiating element (W_0) is positioned on the axis of symmetry ($\rho = 0$). Second points (U_1, V_1, W_1), third points (U_2, V_2, W_2), and forth points (U_3, V_3, W_3) are positioned at same distance from the axis of symmetry ($\rho = \rho_1$, $\rho = \rho_2$, and $\rho = \rho_3$ respectively). ρ_3 is between ρ_{31} and ρ_{max} where $c < \rho_{31} < \rho_{max}$, ρ_2 is between ρ_{21} and ρ_{22}, and ρ_1 is between ρ_{11} and ρ_{12} where $c < \rho_{11} < \rho_{12} < \rho_{21} < \rho_{22} < \rho_3$.

The last control point of the ground (U_3) is positioned on ρ-axis and other control points of the ground are below a specified level ($0 < z_{U_i} < z_{U_{12}}$, $i = 0, 1, 2$). U_0 is also below V_0 ($z_{U_0} < z_{V_0}$). V_0 is below a specified level ($z_{V_0} < z_{V_{11}}$) and other control points of the lower part of radiating element are between $z = z_{V_{11}}$ and $z = z_{V_{12}}$ ($z_{V_{11}} < z_{V_i} < z_{V_{12}}$, $i = 1, 2, 3$). Each control point of the upper part of radiating element is between the corresponding control point of the lower part and $z = z_{max}$ ($z_{V_i} < z_{W_i} < z_{max}$, $i = 0, 1, 2, 3$).

Special kind of spline is used to derive the final profile. This spline replaces each edge of a given polygon by a curve with specified expansion and sharpness which are determined respectively by expansion and sharpness factors assigned to that edge. An expansion and a sharpness factor should be assigned to each control point shown in Fig. 1 ($0 < e_{X_i}, s_{X_i} < 1$, $X \equiv U, V, W$, $i = 0, 1, 2, 3$).

a, b, c, l, t, $\Delta\rho_{max}$, Δz_{max}, $\Delta\rho_{grd}$, $\Delta\rho_{mar}$ Δz_{mar}, ρ_{11}, ρ_{12}, ρ_{21}, ρ_{22}, ρ_{31}, $z_{U_{12}}$, $z_{V_{11}}$, and $z_{V_{12}}$ are constant parameters which are appointed prior to the optimization process according to the dimensions of the feeding cable or connector and the desired sizes of radiating element and ground. ρ_1, ρ_2, ρ_3, ρ_4, z_{U_0}, z_{U_1}, z_{U_2}, z_{V_0}, z_{V_1}, z_{V_2}, z_{V_3}, z_{W_0}, z_{W_1}, z_{W_2}, z_{W_3}, e_{X_i}, and s_{X_i} ($X \equiv U, V, W$, $i = 0, 1, 2, 3$), each could be considered as a constant parameter or an optimization parameter.

A wide variety of shapes could be generated using the proposed scheme, including polygons with sharp edges, polygons with rounded edges and different curved shapes. Therefore, the general description is capable of producing almost all possible shapes for monopole antennas. The proposed scheme never generates self-intersecting or discontinuous shapes. An uninterrupted and smooth transition of radiating pulse from feed line to free-space (or vice versa) could be readily provided by shaping the cross-section of radiating element (especially the lower part of it) and the cross-section of ground in a proper manner, which can be carried out by finding the best positions for control points and the optimum values of spline factors through an optimization process. This general description is compatible with different optimization methods (especially GA) and there is not any possibility for unacceptable shapes to be generated during the optimization process.

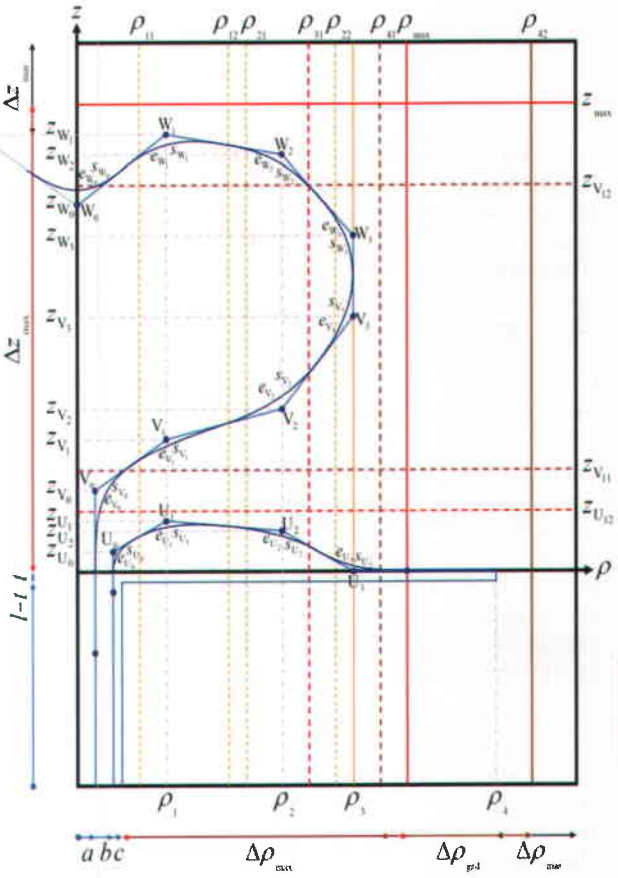

Fig. 1 The proposed scheme to generally describe the geometry of a rotationally-symmetric monopole antenna with finite ground plane.

B. *Electromagnetic Simulator*

The electromagnetic analysis of antennas is carried out by the RSS[1]-FDTD code [15], which is an efficient finite-difference time-domain (FDTD) tool for analyzing the rotationally-symmetric structures. This code is based on the FDTD formulation in cylindrical coordinates taking into account the rotational symmetry of structure and excitation. Therefore, the performed simulations are two-dimensional instead of three-dimensional and the required memory space and CPU-time are significantly low. With low CPU-time requirements, the implementation of different optimization methods (especially the population-based methods) becomes practicable.

The inputs of the RSS-FDTD code include the specifications of the spectral mask and the structure. The code automatically generates an excitation signal which fits into the specified spectral mask. For example, Fig. 2 shows a modulated Gaussian pulse along with its spectral density which fits into the FCC spectral mask for indoor systems.

C. *Objective Function*

The optimization process has two main goals; minimizing the reflection coefficient (i.e. improving the impedance matching) of antennas over the

[1] Rotationally-Symmetric Structures

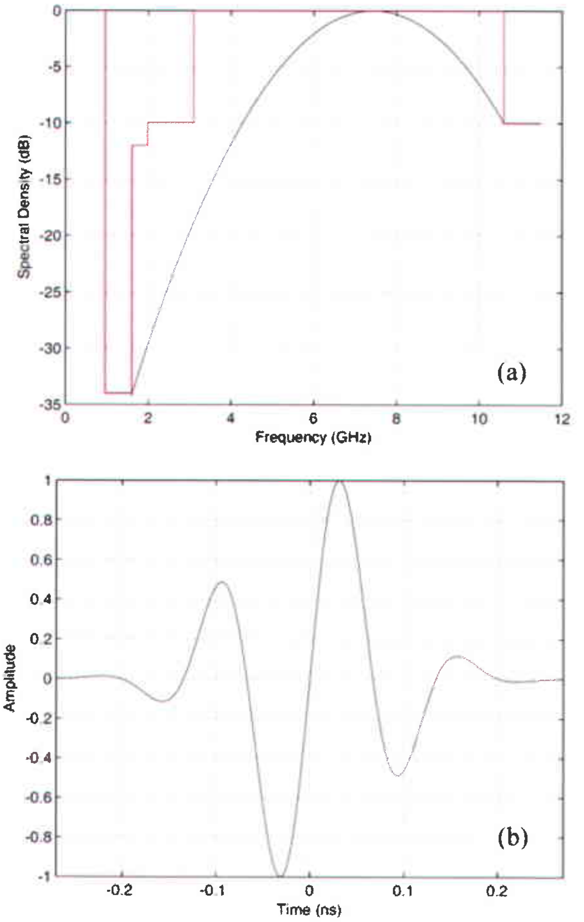

Fig. 2 A modulated Gaussian pulse and (b) its spectral density which fits into the FCC spectral mask for indoor systems.

operating band and reducing the time-domain distortion of radiated pulses. In some cases, the reduction of variations in the energy pattern is added to these goals. The objective function is a weighted sum of terms, each considered to satisfy one of these goals. The term, which is set to satisfy the first goal, is:

$$F_1 = \max_{f\in[f_b, f_e]} \{R(f)\} \quad (1)$$

where f_b and f_e are the lowest and the highest frequencies in the operating band and $R(f)$ is the reflection coefficient. The term considered for the second goal is:

$$F_2 = \frac{\sum_{n=1}^{n_\theta} W(\theta_n).[1 - CF(\theta_n)]}{\sum_{n=1}^{n_\theta} W(\theta_n)} \quad (2)$$

Here $CF(\theta_n)$ is the correlation factor [9] which is the normalized correlation between the input signal of antenna ($s_{in}(t)$) and the signal detected by a virtual probe placed at far-zone along a specified direction ($s_{\theta_n}(t)$) and $W(\theta_n)$ is a weight assigned to that direction. n_θ is the number of specified directions. The weighting for different directions is considered as follows:

$$W(\theta) = \sqrt{1 - \frac{|\theta - \pi/2|}{\pi/2}} \quad (3)$$

The term, which is considered for the reduction of variations in the energy pattern, is:

$$F_3 = \frac{1}{s(n_\theta - 1)} \sum_{n=1}^{n_\theta} |P(\theta_n)| \quad (4)$$

where

$$P(\theta) = 10\log\left[\frac{E(\theta)}{\max_n E(\theta_n)}\right], \quad E(\theta) = \int s_\theta^2(t)dt \quad (5)$$

$P(\theta)$ is the relative average power of pulse in a specified direction which could be expressed in dB. In (4), s is a constant which is set equal to 30.

Finally, the objective function is evaluated as follows:

$$F = c_1F_1 + c_2F_2 + c_3F_3 \quad (6)$$

When optimization is restricted to the main goals, c_1 and c_2 are set equal to 0.65 and 0.35, respectively and the third term is omitted. Otherwise, c_1, c_2, and c_3 are set equal to 0.4, 0.2, and 0.4, respectively.

D. Optimization Procedure

The variety of possible geometries and the high number of optimization parameters raise the possibility of having different optimum designs. In other words, the objective function may have multiple local minimums in the search domain. Consequently, global optimization methods should be used in order to search for the best design. Moreover, the process of calculating the objective function for each antenna structure is relatively complex and lengthy, including the electromagnetic simulation of antenna and the computation of characteristics which are invc (b) n the definition of objective function. Thereft e implementation of heuristic strategies is necessary in order to reduce the overall time needed for the completion of the optimization process. On the other hand, the final stages of optimization with heuristic strategies are subjected to stagnation, so it is better to complete the global optimization by implementing a local optimization method.

In this work, the optimization of UWB antennas is performed by applying a hybrid procedure. First, the global optimization is carried out using the MATLAB GA optimizer [16], [17]. Then, the procedure is completed by a local optimization using the pattern search method [17].

III. Numerical Resuts

In this section, two optimized profiles for UWB monopole antenna with finite ground plane are presented which are obtained by the predescribed optimization process. In both cases, the optimization process is performed to design antennas suitable for UWB indoor applications. Antennas are fed through a 50 Ω coaxial line. The values of Δz_{mar}, $\Delta\rho_{grd}$, and $\Delta\rho_{mar}$ are chosen equal to 2.5 cm, 1.5 cm, and 2.5 cm, respectively.

During the GA search, all expansion and sharpness factors are fixed equal to 1 and 0.5, respectively. But during the pattern search, these factors are considered as tunable parameters. To calculate the value of objective function, f_b and f_e in (1) are set equal to 3.1 GHz and 10.6 GHz, respectively. Also, the values of θ_n in (2) and (5) are chosen equal to 90°, 60°, and 30°.

The first antenna profile is obtained considering a flat ground and both $\Delta\rho_{max}$ and Δz_{max} equal to 2.5 cm. Moreover, optimization is restricted to the main goals. Fig. 3 shows the first antenna profile. The diameter and height of antenna and the diameter of ground plane are 3.56 cm, 2.47 cm, and 7.58 cm, respectively. Fig. 4 presents the return loss of antenna in 3.1-10.6 GHz band calculated by RSS-FDTD and CST [1] Microwave Studio software. It is necessary to note that the CST software is not used in the optimization process. The CST calculated data are only prepared for the final optimized antenna. The widest difference between the two sets of data is less than 3.5 dB. The maximum return loss in this band is -18.3 dB. The radiated waveforms at $\theta = 90^\circ$, $\theta = 60^\circ$ and $\theta = 30^\circ$ and their spectral density are shown in Fig. 5, Fig. 6 and Fig. 7, respectively. Fig. 8 shows the correlation factor at different elevation angles. The correlation factor is above 0.9 at most angles and it is above 0.95 between 31° and 138°. Fig. 9 presents the energy pattern of the antenna. The average power of pulse at $\theta = 90^\circ$ is 5.8 dB less than maximum.

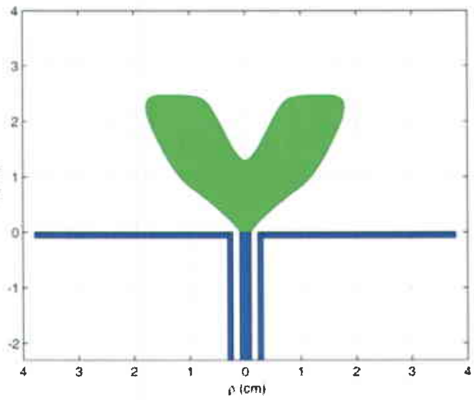

Fig. 3 The first optimized profile for UWB monopole antenna with finite ground plane.

[1] Computer Simulation Technology

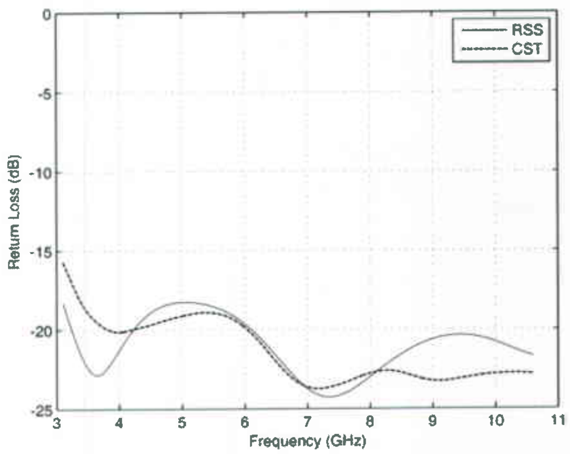

Fig. 4 Return loss of the first optimized antenna calculated by RSS-FDTD (solid line) and CST Microwave Studio (dashed line).

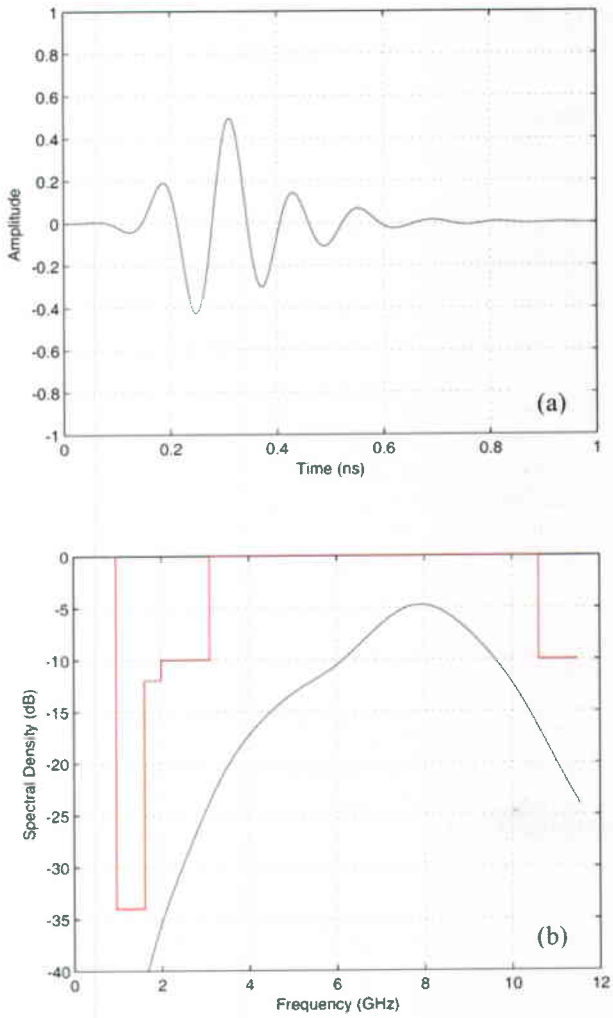

Fig. 5 (a) Radiated waveform of the first optimized antenna at $\theta = 90^\circ$ along with (b) its spectral density.

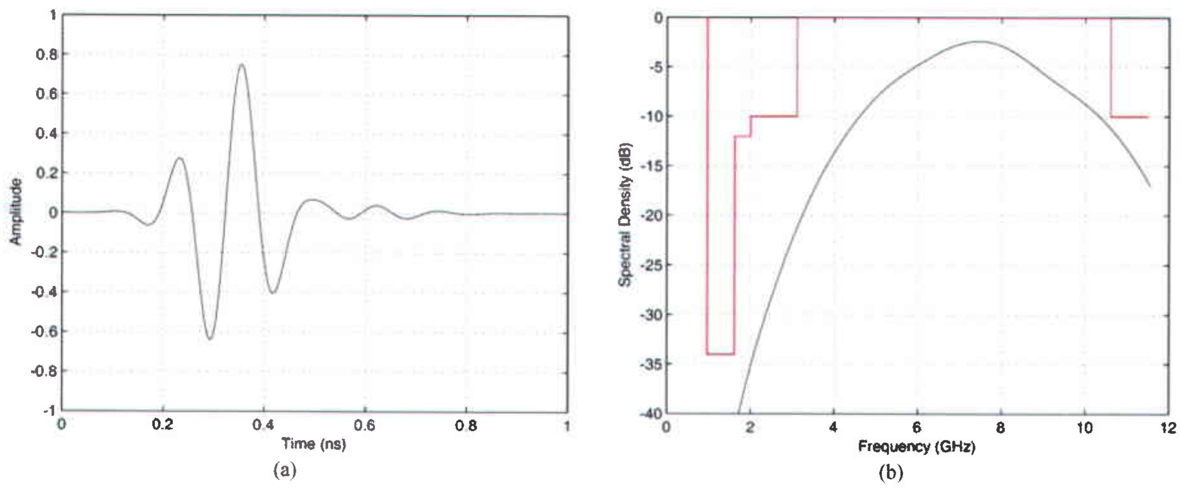

Fig. 6 (a) Radiated waveform of the first optimized antenna at $\theta = 60^{\circ}$ along with (b) its spectral density.

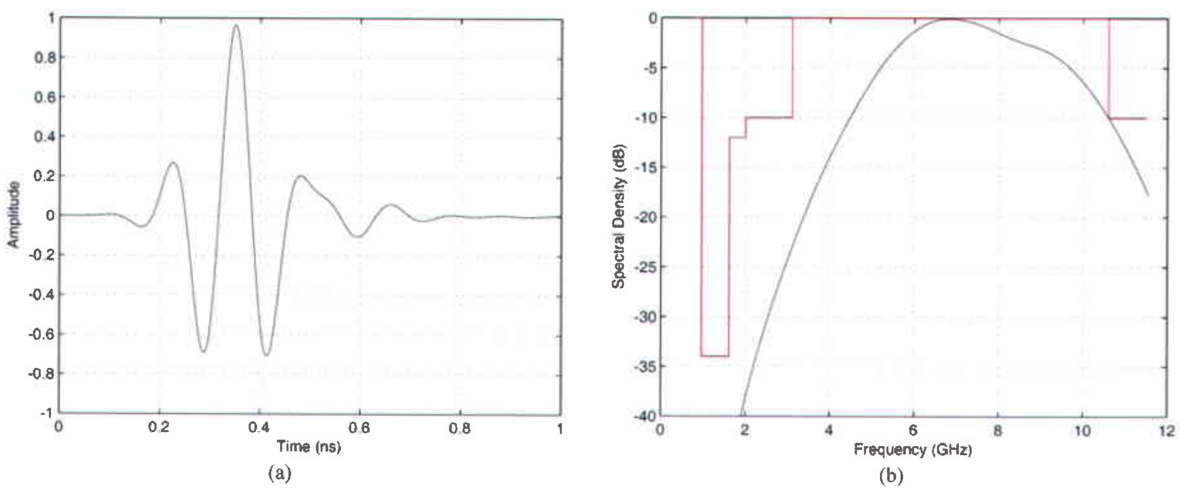

Fig. 7 (a) Radiated waveform of the first optimized antenna at $\theta = 30^{\circ}$ along with (b) its spectral density.

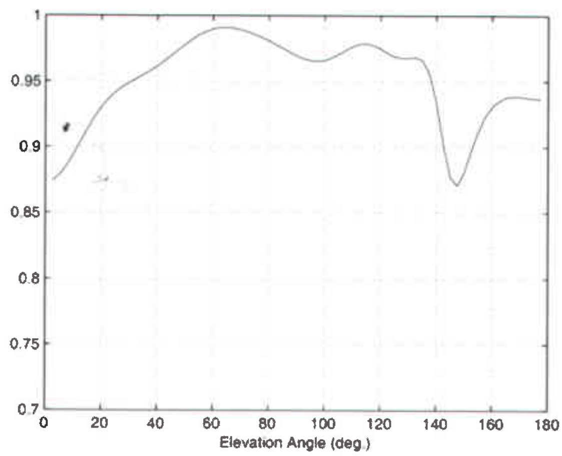

Fig. 8. Correlation factor for the first optimized antenna as a function of elevation angle.

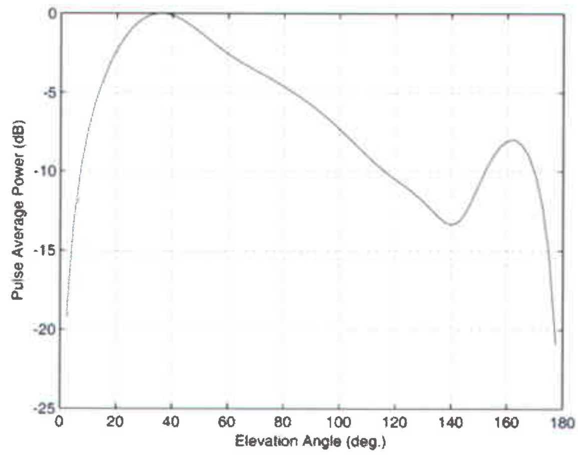

Fig. 9. Energy pattern of the first optimized antenna.

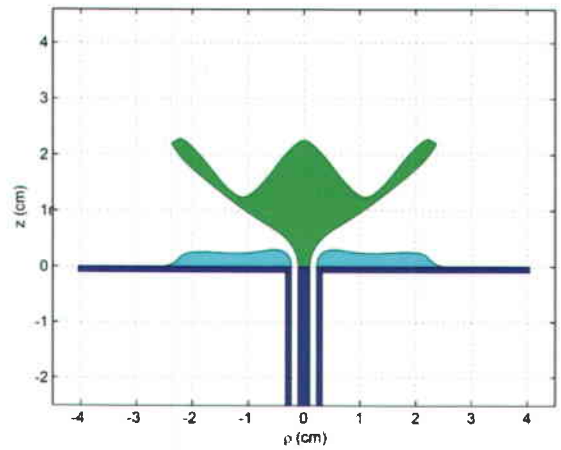

Fig. 10. The second optimized profile for UWB monopole antenna with finite ground plane.

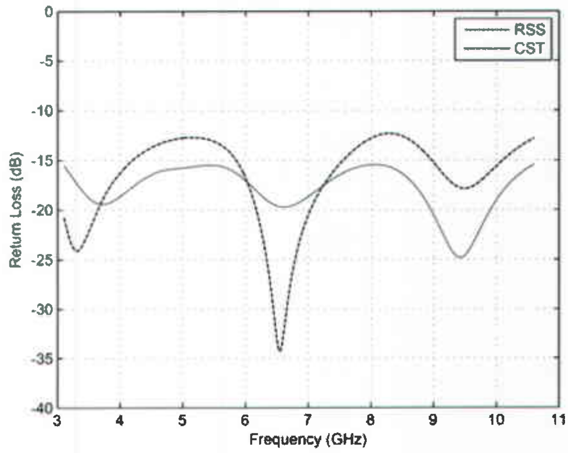

Fig. 11. Return loss of the second optimized antenna.

The second antenna profile is obtained considering a shaped ground and the same values for $\Delta\rho_{max}$ and Δz_{max} as in the previous case. In this case, the reduction of variations in the energy pattern is added to the optimization goals. Fig. 10 shows the second antenna profile. Antenna has a diameter and height of 4.73 cm and 2.28 cm, respectively. The diameter of ground plane is 8.08 cm. The return loss of antenna is shown in Fig. 11. The maximum return loss in 3.1-

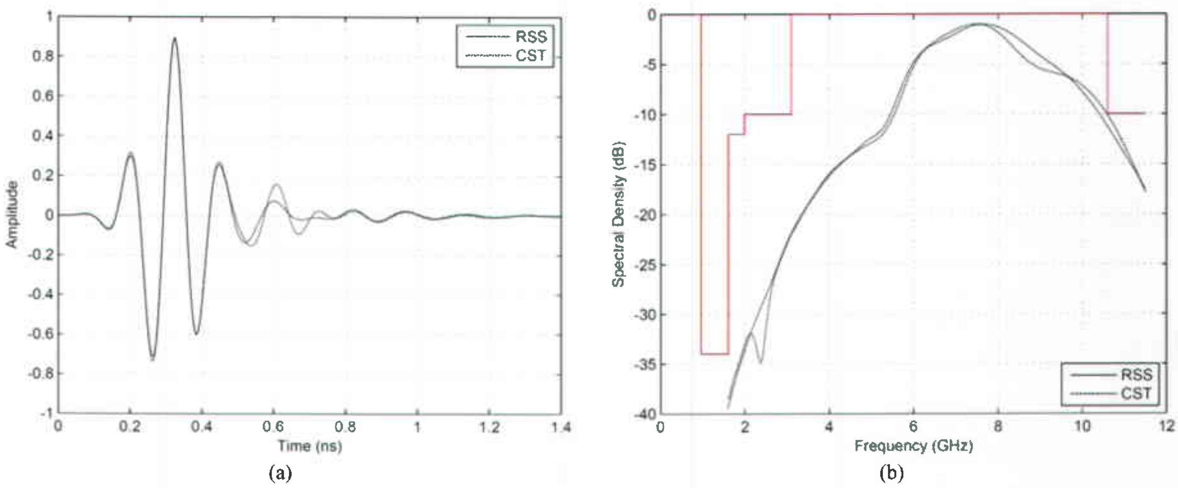

Fig.12. (a) Radiated waveform of the second optimized antenna at $\theta = 90^{\circ}$ along with (b) its spectral density.

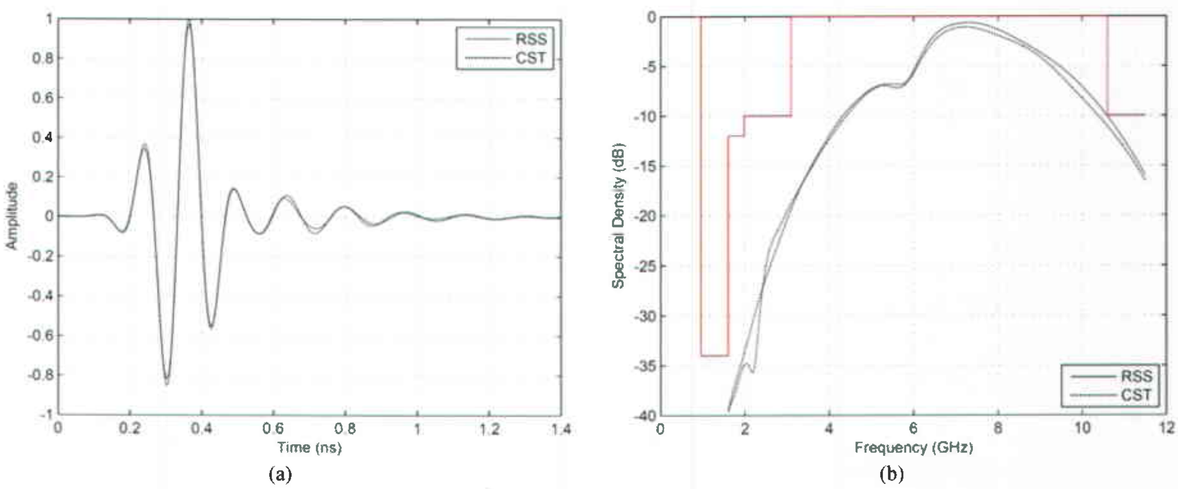

Fig. 13. (a) Radiated waveform of the second optimized antenna at $\theta = 60^{\circ}$ along with (b) its spectral density.

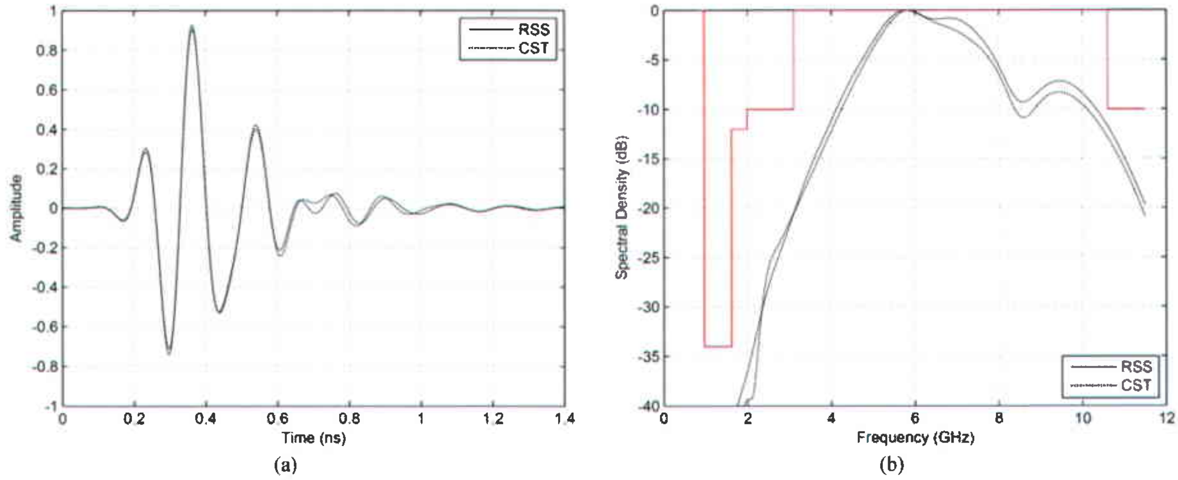

Fig. 14. (a) Radiated waveform of the second optimized antenna at $\theta = 30^\circ$ along with (b) its spectral density.

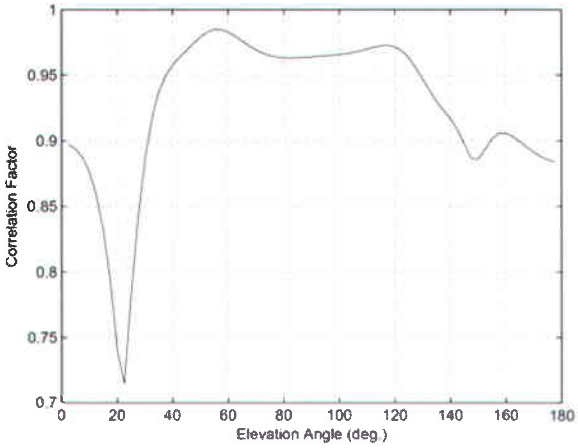

Fig. 15. Correlation factor for the second optimized antenna as a function of elevation angle.

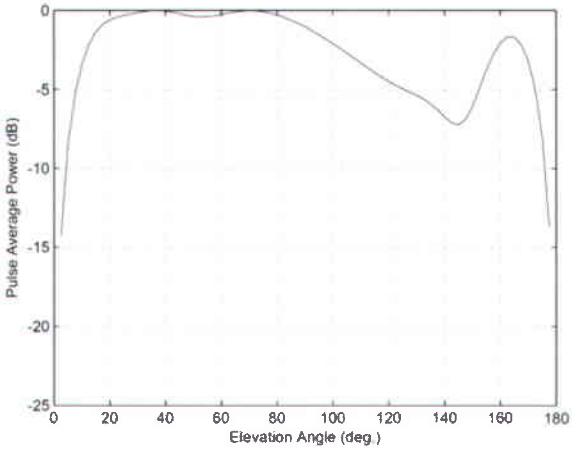

Fig. 16. Energy pattern of the second optimized antenna.

10.6 GHz band is -15.4 dB. The two sets of data shown in Fig. 11 exhibit similar variations throughout the frequency band. The difference between the two sets of data is caused by 3D-rectangular modeling of antenna in CST software which doesn't accurately taking into account the rotational symmetry of structure and excitation. The radiated waveforms at $\theta = 90^\circ$, $\theta = 60^\circ$, and $\theta = 30^\circ$ (calculated by RSS-FDTD and CST Microwave Studio) and their spectral density are shown in Fig. 12, Fig. 13 and Fig 14, respectively. There is excellent agreement between RSS and CST calculated data. Fig. 15 presents the correlation factor at different elevation angles. The energy pattern of the antenna is shown in Fig. 16. In this case, the average power of pulse at $\theta = 90^\circ$ is only 1.0 dB less than maximum which shows 4.8 dB improvement compared to the first antenna. Fig. 17 shows the radiation (directivity) pattern of the antenna at 6.85 GHz.

Fig. 18 shows a pair of second optimized antennas placed 50 cm away from each other in free space which are operating as transmitter and receiver. Fig. 19 presents the signal at output terminals of the receiving antenna calculated by means of CST Microwave Studio software. The spectral density of

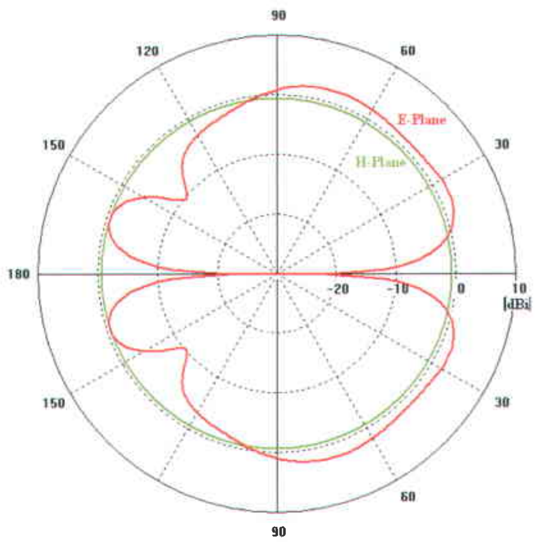

Fig. 17. Radiation (directivity) pattern of the second optimized antenna at 6.85 GHz.

Fig. 18. A pair of second optimized antennas placed 50 cm away from each other in free space which are operating as transmitter and receiver.

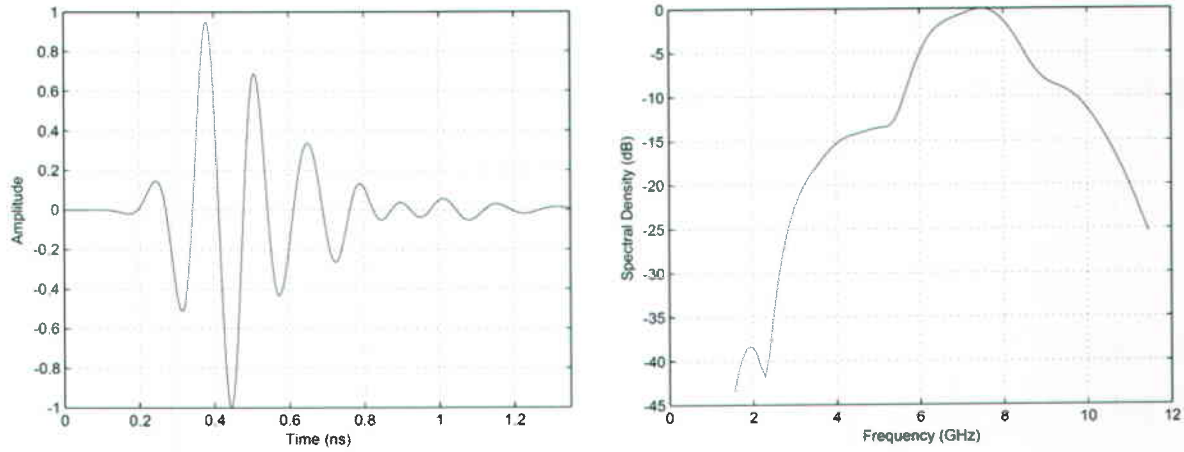

(a) (b)

Fig. 19. (a) Signal at the output terminals of the receiving antenna (Fig. 18) and (b) its spectral density.

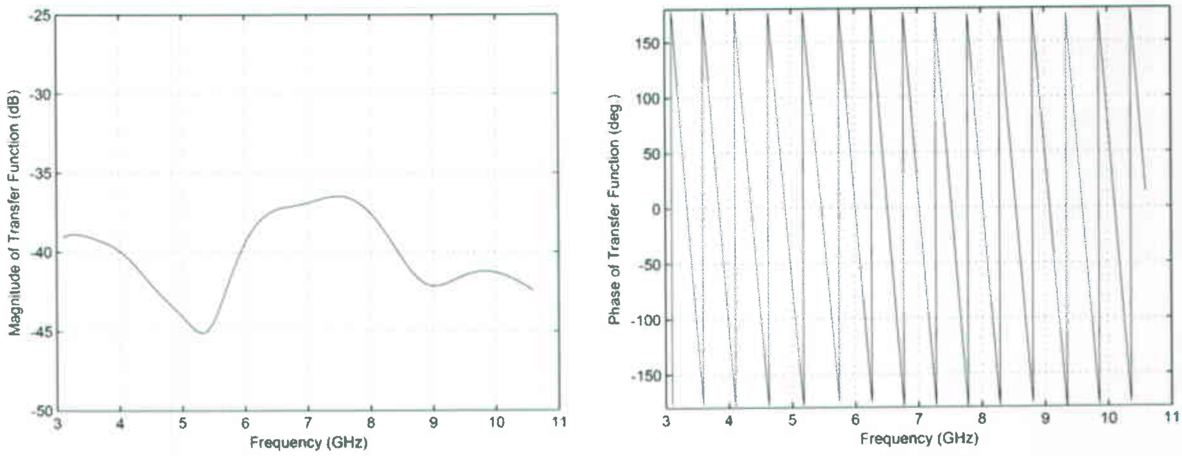

(a) (b)

Fig. 20. Transfer function of the two-antenna system shown in Fig. 18. (a) Magnitude and (b) phase.

signal is also shown in this Figure. The normalized correlation between the input signal of transmitting antenna and the output signal of receiving antenna is 0.88. The magnitude and phase of transfer function (S_{21}) are shown in Fig. 20. The corresponding group delay (τ_g) is shown in Fig. 21. The widest variations of $|S_{21}|$ and τ_g in 3.1-10.6 GHz band are less than 8.6 dB and 0.39 ns, respectively.

IV. Conclusions

The numerical results show the reliability and effectiveness of the whole optimization process. These results also show considerable improvement regarding antenna size and operational characteristics in comparison with similar antennas reported in the literature.

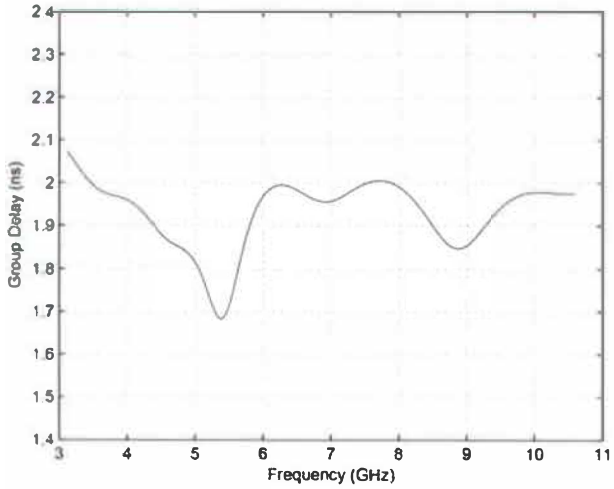

Fig. 21. Group delay in the two-antenna system shown in Fig. 18.

REFERENCES

[1] Federal Communication Commission, First Report and Order, "Revision of part 15 of the commission's rules regarding ultra-wideband transmission systems," FCC 02-48, Apr. 2002.

[2] O. E. Allen, D. A. Hill, and A. R. Onderjka, "Time-domain antenna characterizations," *IEEE Trans. Electromagn. Compat.*, vol. 35, no. 3, pp. 339-346, Aug. 1993.

[3] J. S. McLean, H. Foltz, and R. Sutton, "Pattern descriptors for UWB antennas," *IEEE Trans. Antennas Propagat.*, vol. 53, no. 1, pp. 553-559, Jan. 2005.

[4] G. Lu, S. von der Mark, I. Korisch, L. J. Greenstein, and P. Spasojevic´, "Diamond and rounded diamond antennas for ultrawide-band communications," *IEEE Antennas Wireless Propagat. Lett.*, vol. 3, pp. 249-252, 2004.

[5] T. Nakamura and H. Iwasaki, "Planar monopole antenna having a band-notched characteristic for UWB," in *Proc. IEEE Antennas and Propagation Society Int. Symp.*, 2006, pp. 4641-4644.

[6] T. Yang, S. Y. Suh, R. Nealy, W. A. Davis, and W. L. Stutzman, "Compact antennas for UWB applications," *IEEE Aerospace Electronic Systems Mag.*, vol. 19, May 2004.

[7] D. Ghosh, A. De, M. C. Taylor, T. K. Sarkar, M. C. Wicks, and E. L. Mokole, "Transmission and reception by ultra-wideband (UWB) antennas," *IEEE Antennas Propagat. Mag.*, vol. 48, no. 5, pp. 67-99, Oct. 2006.

[8] A. Alomainy, Y. Hao, C. G. Parini, and P. S. Hall, "Comparison between two different antennas for UWB on-body propagation measurements," *IEEE Antennas Wireless Propagat. Lett.*, vol. 4, pp. 31-34, 2005.

[9] N. Telzhensky and Y. Leviatan, "Novel method of UWB antenna optimization for specified input signal forms by means of genetic algorithm," *IEEE Trans. Antennas Propagat.*, vol. 54, no. 8, pp. 2216-2225, Aug. 2006.

[10] N. Telzhensky and Y. Leviatan, "Planar differential elliptical UWB antenna optimization," *IEEE Trans. Antennas Propagat.*, vol. 54, no. 11, pp. 3400-3406, Nov. 2006.

[11] J. Kim, T. Yoon, J. Kim, and J. Choi, "Design of an ultra wide-band printed monopole antenna using FDTD and genetic algorithm," *IEEE Microwave Wireless Components Lett.*, vol. 15, no. 6, pp. 395-397, June 2005.

[12] J. Martínez-Fernández, J. M. Gil, and J. Zapata, "Ultrawideband optimized profile monopole antenna by means of simulated annealing algorithm and the finite element method," *IEEE Trans. Antennas Propagat.*, vol. 55, no. 6, pp. 1826-1832, June 2007.

[13] L. Lizzi, F. Viani, R. Azaro, and A. Massa, "Optimization of a spline-shaped UWB antenna by PSO," *IEEE Antennas Wireless Propagat. Lett.*, vol. 6, pp. 182-185, 2007.

[14] P. Cerny, M. Mazanek, "Simulated transient radiation characteristics of optimized ultra wideband printed dipole antennas," in *Proc. Radioelektronika Int. Conf.*, Apr. 2007, pp. 1-6.

[15] K. Paran and M. Kamyab, "Electromagnetic radiation from vertical dipole antennas near air-lossy soil interface—A finite-difference time-domain simulation," *International Journal of Numerical Modeling: Electronic Networks, Devices and Fields, John Wiley & Sons Ltd*, vol. 18, Issue 2, pp. 119-132, March/April 2005.

[16] Y. Rahmat-Samii and E. Michielssen, *Electromagnetic optimization by genetic algorithms*. New York: John Wiley & Sons, 1999.

[17] Genetic algorithm and direct search toolbox user's guide. MathWorks.

Kian Paran was born in Tehran, Iran in 1972. He received the M.S. degree in Electrical Engineering from the University Tehran in 1998 and the Ph.D. degree in Electrical Engineering from the K. N. Toosi University of Technology, Tehran, Iran in 2005. He is currently an Assistant Professor at the Communications Technology Institute of Iran Telecommunication Research Center (ITRC). His research interests are in computational electromagnetics (especially time-domain methods), optimization of electromagnetic structures and empirical methods, radio-wave propagation (physics and path-loss prediction methods) and UWB antennas.

Masoum Fardis received Ph.D. degree in MMIC's from I.I.T.Delhi and worked in various fields of MMIC's applications including Fin-line, Microwave Theory and Antennas. In.1994 he joined as a head of radio and optic division and also data & multiplex department in I.T.R.C Tehran Iran. From 2003 to 2006 he was appointed as a deputy of research and technology and acting director of I.T.R.C,he was also project manager of second operator in cellular network of Iran. Current academic interests include variety of research issues associated with I.C.T including Ultra wide band, Ad-hoc networking and designing added-value services systems.

Ali Abolghasemi- He is faculty member of Communication Technology Institute in Radio Communication group of ITRC (Iran Telecommunication Research System). He received his B.Sc. and M.Sc. degrees of Electrical and Telecommunications Engineering from K. N. Toosi University of Technology, Tehran, Iran, in 1991 and 1995, respectively. From 1997 until 2007 he has been working in switching and signaling in fixed and mobile communication system (ISDN, 2G, and 3G). Current field of his research include 3G and beyond mobile and wireless communication systems.